Lab on a Chip

Cite this: *Lab Chip*, 2011, **11**, 3689

www.rsc.org/loc

PAPER

Microfluidic chamber arrays for whole-organism behavior-based chemical screening†

Kwanghun Chung,‡[a] Mei Zhan,‡[b] Jagan Srinivasan,[c] Paul W. Sternberg,[c] Emily Gong,[a] Frank C. Schroeder[d] and Hang Lu*[ab]

Received 10th May 2011, Accepted 30th August 2011
DOI: 10.1039/c1lc20400a

The nematode *Caenorhabditis elegans* is an important model organism in genetic research and drug screening because of its relative simplicity, ease of maintenance, amenability to simple genetic manipulation, and relevance to human biology. However, their small size and mobility make nematodes difficult to physically manipulate, particularly with spatial and temporal precision. We have developed a microfluidic device to overcome these challenges and enable fast behavior-based chemical screening in *C. elegans*. The key components of this easy-to-use device allow rapid loading and housing of *C. elegans* in a chamber array for chemical screening. A simple two-step loading process enables simultaneous loading of a large number of animals within a few minutes without using any expensive/active off-chip components. In addition, chemicals can be precisely delivered to the worms and exchanged with high temporal precision. To demonstrate this feature and the ability to measure time dependent responses to chemicals, we characterize the transient response of worms exposed to different concentrations of anesthetics. We then use the device to study the effect of chemical signals from hermaphrodite worms on male behavior. The ability of the device to maintain a large number of free moving animals in one field of view over a long period of time permits us to demonstrate an increase in the incidence of a specific behavior in males subjected to worm-conditioned medium. Because our device allows monitoring of a large number of worms with single-animal resolution, we envision that this platform will greatly expedite chemical screening in *C. elegans.*

Introduction

Multicellular organisms, such as *Caenorhabditis elegans*, *Drosophila melanogaster*, and *Danio rerio*, have been crucial in elucidating fundamental biological mechanisms and human disease pathogenesis.[1–8] In particular, the conservation of many genes and biological mechanisms between *C. elegans* and humans, together with the simplicity and ease of their maintenance, make *C. elegans* an effective *in vivo* model for behavioral analysis in response to chemical stimuli.[9–14] These assays are typically done by establishing a concentration gradient of chemicals from a point source in an agar plate and observing the final distribution of animals on the plate or measuring the amount of time spent in each region.[14] Although, these assays are informative, diffusion of the chemicals into the agar surface and evaporation make it difficult to characterize the actual concentration of chemical that the worms are exposed to. In addition, these traditional assays do not allow temporal control in the delivery of chemicals. Another common method is to deliver chemicals using a pipette to a worm partially immobilized by glue and observe its behavioral response[15] or calcium transients in the neurons.[16] While this method is advantageous in that it allows temporal control in delivering chemicals, gluing down or trapping the worm limits the measurable behavioral outputs. In addition, chemicals in the glues and mechanical stimulation from being immobilized may also affect neuronal activity. Moreover, both methods require painstaking manual handling of the micron-scale nematode, which makes chemical screening laborious and susceptible to inconsistencies in handling. These disadvantages often preclude certain types of experimentation altogether.

Recently, significant progress has been made in overcoming these limitations. Ryu *et al.* and Luo *et al.* developed a single-worm microdroplet assay to study the olfactory sensory and

[a]*School of Chemical & Biomolecular Engineering, Georgia Institute of Technology, 311 Ferst Dr, NW, Atlanta, GA, 30332-0100, USA. E-mail: hang.lu@gatech.edu; Fax: +1-404-894-8473; Tel: +1-404-894-8473*
[b]*Interdisciplinary Program of Bioengineering, Georgia Institute of Technology, 311 Ferst Dr, NW, Atlanta, GA, 30332-0100, USA. E-mail: hang.lu@gatech.edu; Fax: +1-404-894-8473; Tel: +1-404-894-8473*
[c]*MC156-29, Biology Division, California Institute of Technology, 1200 East California Blvd, Pasadena, CA, 91125, USA*
[d]*Boyce Thompson Institute and Department of Chemistry and Chemical Biology, Cornell University, Ithaca, NY, 14853, USA*

† Electronic supplementary information (ESI) available. See DOI: 10.1039/c1lc20400a

‡ These authors contributed equally.

thermotactic behaviors of *C. elegans* by measuring motile responses to temporal variation of odorants or temperature stimuli.[17,18] In their assays, single worms were manually placed in droplets. Heating blocks provided thermal stimuli and chemical stimuli were provided by airstreams carrying a defined vapor concentration of volatile odors. By confining worms in a grid of droplets, this method allows a large number of worms to be simultaneously monitored over an extended period of time. Shi *et al.* took a similar approach, but utilized droplet-based microfluidic technology to automatically load worms in the droplets.[19] Using a microfluidic device, they were able to encapsulate *C. elegans* into a parallel series of droplets in $\sim$ 10 mins with more than 60% probability. Combining automation and temporal control, Chokshi *et al.* developed an automated microfluidic system to simultaneously monitor worm neuronal activity in respond to chemical stimuli.[20] This system allows precise delivery of chemicals to the nose of partially physically restrained worms with high temporal resolution. For long term longitudinal studies, Hulme *et al.* also developed a microfluidic device for confining individual worms in sixteen separate microfabricated chambers.[21] A branching network of delivery channels with prefabricated screw valves was used to load worms into the device one at a time at the rate of approximately 1 min per worm.

A device to trap individual *C. elegans* within chambers and individually address each chamber with chemical compounds has also be previously described by Rohde *et al.*[22] While this device has the advantage of permitting multiple chemical conditions to be assayed on the same chip, the sample sizes per condition and the number of worms that can be viewed simultaneously is limited by the multiple control lines needed for individual addressing of the chambers. Recently, another screening platform has been introduced that uses an electric field to guide worms into and out of a drug in order to study worm behavior.[23] This device permits the study of behavior in response to well controlled doses of specific chemicals. However, sample sizes and the throughput for each condition are limited by the difficulty in loading, controlling and monitoring the worms in multiple behavioral channels at the same time. Therefore, although these devices provide the means to perform well controlled chemical screening based on less noisy physiological readouts that require lower sample sizes, their inability to assay a large number of worms quickly render them non-ideal for behavioral assays, where sample sizes of 20–30 or more worms are commonly used.[24–26]

Although these recent innovations advance the goal of efficient chemical screening using *C. elegans*, there is still a need for a technology that simultaneously fulfills the following functions and criteria: (1) robust and efficient worm handling; (2) ability to monitor behavior of a larger number of worms simultaneously; (3) temporal control in delivering non-volatile chemicals comprising most of metabolites and drug candidates; (4) robust and easy fabrication; and (5) ease of use for non-experts. Here, we present a microfluidic platform to enable rapid chemical screening based on whole-organism behavioral responses. The easy-to-use PDMS (polydimethylsiloxane) device includes essential components that allow simultaneous loading and monitoring of the phenotypic responses of up to forty-eight worms in the field of view. Chemicals can be delivered to the chambers in a quick and fully controllable manner. In addition, the operation of the one-layer PDMS device is simple and does not require any expensive/active off-chip components.

We demonstrate the capabilities of our device in two biological experiments. As a first test to demonstrate the ability of our device to facilitate high throughput characterization of transient behavioral responses, we assess the initial responses of *C. elegans* to different concentrations of sodium azide, a commonly used anesthetic. We then applied our device to study signaling molecules that regulate development and mating of *C. elegans*.[27–33] It has been previously demonstrated that male worms dwell longer in areas treated with media preconditioned by young adult hermaphrodites.[27,28] Here, we use the power of our device to perform longitudinal behavioral tracking of a large number of individual worms to investigate behavioral responses of *C. elegans* males to hermaphrodite-conditioned medium.

Experimental

Design of the microfluidic device

Fig. 1 shows the design of the microfluidic device. The one-layer PDMS device consists of a serpentine channel and an array of circular chambers that connect each row of the serpentine channel to the next. The 500-μm wide serpentine channel carries worms and media throughout the device. It has two separate inlets, a large inlet (I1) for worm entry and a small inlet (I2) for media exchange, and one outlet (O). The 1.5 mm wide circular chambers house individual worms to allow monitoring of the behavioral responses of single, identifiable animals. To maximize the number of the chambers in the field of view, we minimized the distances between the chambers and densely arrayed 48 chambers in 8 (column) $\times$ 6 (row) format (Fig. 1a). When $\sim$7x magnification is used, which is high enough to read out many aspects of behavioral response of young adult worms, all 48 chambers can be monitored in the field of view (18.13 mm $\times$ 13.54 mm).

Each chamber includes novel components to enable rapid loading of single worms in the chambers, uniform chemical delivery to the chambers, and confinement of the worm in the chamber for the entire assay (Fig. 1b). Specifically, worm loading areas (b) are separated from the main worm housing chamber (d) by a narrow "stopper" region (c). These features permit single worms to be trapped in the loading areas awaiting entry into the main chamber. The stopper is constructed with a thin, wide base (light blue in Fig. 1b), permitting large deformations that allow sufficient space for worm passage when pressurized. Once worms pass through the stopper into the chamber, a collection of small outlet channels (e) that converge into a chamber outlet (f) into the next row of the main serpentine channel serve both the functions of retaining the worms in the chamber and permitting fluid flow across the channel for both worm loading and media exchange. All the features are fabricated in PDMS with a mixing ratio of 20 : 1 to make it highly deformable (Fig. 1c). The upper part of the device that surrounds the holes is made of PDMS with mixing ratio of 10 : 1 for mechanical integrity.

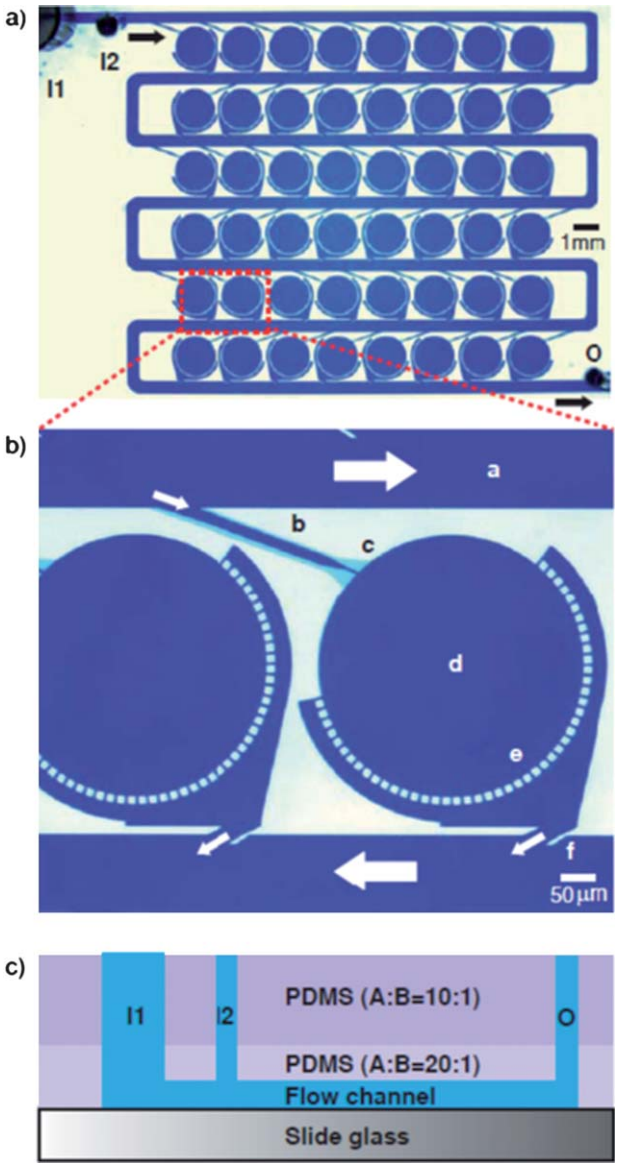

Fig. 1 Optical micrographs of the worm chamber array device. a) Dye-filled image of the device showing array of 48 circular chambers connected to the serpentine channel. Black arrows represent flow direction. I1, worm inlet; I2, chemical inlet; O, outlet. b) Zoomed in image of the boxed region in **a** showing microfluidic components to enable high-throughput single worm loading and chemical delivery: a, serpentine channel; b, single worm loading channel; c, stopper; d, circular chamber; e, diverging channels; f, chamber outlet. White arrows represent flow direction. c) Schematic drawing showing cross-section of the device.

Device fabrication

Soft lithography was used to fabricate devices in PDMS (Dow Corning Sylgard 184, Midland, MI).[34] First, to fabricate the mold, SU8-2010 and SU8-2050 were spin-coated on a wafer for 10 μm and 80 μm layers, respectively. The features on transparency masks were transferred to the SU8-coated wafer by standard UV photolithography. The wafer surface was treated with tridecafluoro 1,1,2,2-tetrahydrooctyl-1-trichlorosilane vapor (United Chemical Technologies, Inc, Bristol, PA) to facilitate release of PDMS from the mold. To form a ~3mm-thick PDMS layer on top of the mold, a mixture of PDMS (part A and B in a 20 : 1 ratio) was poured on the mold. The mold was then degassed for an hour to remove air bubbles. After partially curing the first layer PDMS for 30 min at 75 °C, PDMS (part A and B in a 10 : 1 ratio) was poured on the mold to form 5 mm-thick layer and then cured for 2 h at 75 °C. After peeling off the 8 mm-thick PDMS, the devices were cut into shape and access holes were punched in the PDMS before the devices were bonded to the slide glass. 10 gauge needles (McMaster-Carr, Elmhurst, IL) were use to punch the large worm inlet and 19 gauge needles were used to punch the chemical inlet and the outlet.

Operation of the microfluidic device

The process of loading worms into the microfluidic device is shown in Fig. 2. Initially, the media inlet (I2) was blocked by small plug inserted into the PDMS and the outlet (O) was closed by a valve on the outlet tubing (Fig. 2a). After a liquid suspension of worms was deposited into the worm inlet (I1), the valve on the outlet tubing was opened and a ~50 cm height difference between the worm inlet and the end of the outlet was used to drive the flow of the liquid suspension through the device (Fig. 2b). After all of the worms had either entered the loading areas before the chambers or exited the device through the outlet (Fig. 3a), the device was quickly pressurized *via* the insertion of a large plug into the worm inlet (Fig. 3b). This quick pressurization temporarily allowed the stopper region of each chamber to deform enough to permit worms to enter the chambers.

After worm loading, the media inlet (I2) was used to rapidly exchange the media in each of the chambers in order to facilitate the addition, removal, or exchange of chemical stimuli. To exchange media, the outlet tubing valve was closed and the small plug is removed from the media inlet. A small drop (~50 μL) of the new media was placed on top of the media inlet and the outlet valve was opened for ~15 s to allow the new media to flow through the device.

C. elegans strains and sample preparation

Wild-type *C. elegans* (N2 Bristol) and CB1490 *him-5*(*e1490*) were used in our experiments. All strains were maintained at 20 °C. For all the assays, age-synchronized young adult worms were prepared as follows: embryos were obtained by bleaching adults using a solution containing about 1% NaOCl and 0.1 M NaOH, washed and allowed to hatch in M9 buffer, and cultured at 20 °C on Nematode Growth Medium (NGM) plates seeded with OP50. To generate the liquid suspension of worms used in each experiment, ~100 young adult worms were washed and suspended in M9 solution containing 0.02 wt% Triton X100 as a surfactant.

All experiments with live animals were performed in compliance with the relevant laws and institutional guidelines.

Confocal imaging of the cross-section of the stopper

To characterize the deformation of the stopper that prevents worms from entering the chambers prior to pressurization, we filled the device with fluorescent dextran (molecular weight 70,000 Da Oregon Green; Invitrogen) solution and imaged cross-section of the stopper at different pressures using confocal microscopy (Zeiss LSM 510 VIS Confocal Microscope). The

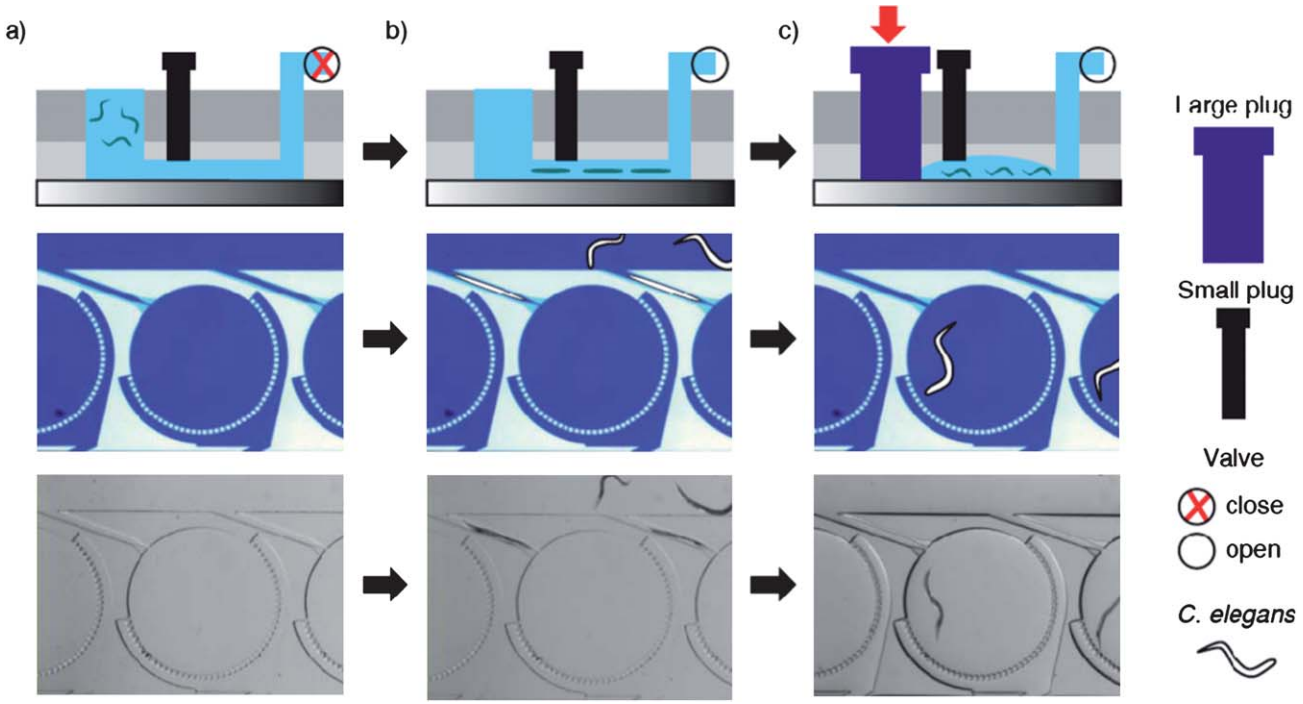

Fig. 2 Device operation process: top, schematic drawing of the cross-section of the device; middle, illustration of single circular chamber; bottom, optical micrographs of the single circular chamber. a) After filling the device with buffer, outlet valve is closed, and worm suspension is pipetted in the worm inlet. b) To gravity load the worms in the single worm loading channels, outlet valve is open. c) Once the worms are in the single loading channels, the large plug is rapidly inserted into the worm inlet. This applies pressure to expand the stopper and push the worms through the stopper and into the chambers.

device was pressurized through the outlet while both inlets are plugged to maintain the pressure in the device during imaging. In actual device operation, the device expands when the plug is inserted and quickly shrinks back to initial status because the outlet is open to air. Therefore, it is challenging to image the actual cross-sectional profile using confocal microscopy, which takes minutes to image the cross section. To get an idea of the maximum stopper expansion in actual device operation, we closed the outlet and inserted the large plug. Then, the cross-section was imaged as before.

Behavior assay and image acquisition

N2 (for anesthetic response experiments) or *him-5* (for male response experiments) young adults were loaded in the devices as described previously. After loading, fresh M9 without Triton X was introduced and the loaded worms were allowed to rest for 2 min. Then, we captured images of the worms swimming in M9 at an acquisition rate of 15 fps with an Infinity 2 CCD camera (1.4 Megapixel CCD monochrome camera) (Electron Microscopy Sciences, Hatfield, PA), mounted on a Zeiss Stemi SV11

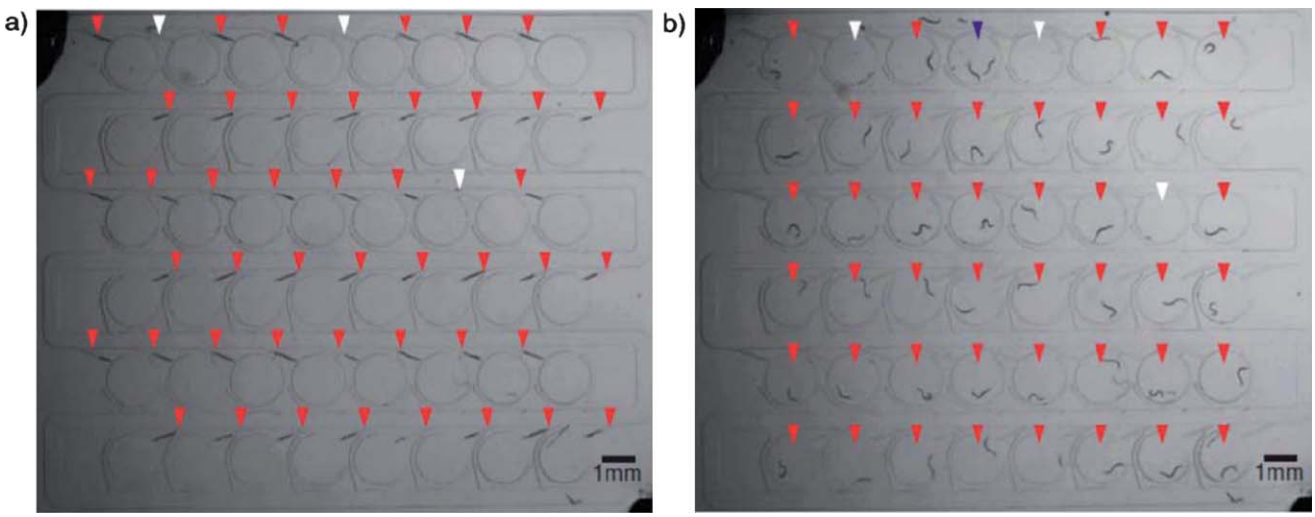

Fig. 3 Optical photographs of *C. elegans* loaded in the single worm loading channels (a) and in the circular chambers (b). Red arrow head, successfully loaded single worms; white arrow head, empty channels/chambers; blue arrow head, multiple worms in single chambers.

dissecting microscope (Carl Zeiss Instruments, Germany). The magnification was set such that all the chambers filled the field of view (18.13 mm × 13.54 mm). For the anesthetic experiments, 2 min of M9 data was acquired before sodium azide was introduced. Behavior after the introduction of sodium azide was then recorded for 5 min. For the male behavioral response experiments, 3 min of M9 data was acquired before hermaphrodite-conditioned medium was delivered and the subsequent behavior of the worms was monitored for another 3 min. After these 3 min of data collection, the media was exchanged for fresh M9 and another 3 min of data was acquired. Once the assay was over, 10 mM sodium azide was introduced to immobilize the worms and then each worm was examined under higher magnification to determine the sex of individual worms. The hermaphrodite-conditioned medium used in these studies was prepared as described in previous publications.[27–33]

Image processing

The captured images were analyzed with code developed in MATLAB®. Each chamber was isolated and analyzed individually. First, features outside of the circular chamber were removed. Thresholding was then employed to segment out the worm body, which is substantially darker than the surrounding fluid. Using the resulting binary image, we find the eccentricity of an ellipse with the same second moments as the area occupied by the worm. Since the eccentricity is a measure of worm elongation, body bending during swimming causes periodic decreases in the eccentricity parameter. We measure body bending frequency for each worm by assessing the frequency of these decreases.

To identify the male specific behavior shown in Fig. 6a, a circular Hough transform was performed on the original grayscale image in order to identify circles formed by tail coiling in the worm. A combination of the Hough transform circle identification result, eccentricity, and temporal relationship to other frames identified as male specific behavior was then used to identify incidences of this behavior in all of the video frames captured for each worm.

Results and discussion

Device operation mechanism

For robust and efficient worm handling, we developed a simple, two-step loading process that allows simultaneous loading of a large number of chambers with single worms within ~3 min. As shown in Fig. 2, the operation of the device only requires the device, a small plug (0.90 mm in OD), a large plug (2.77 mm in OD), and an on/off valve for the outlet tubing. The worm suspension loaded in the large inlet is introduced into the device by the pressure difference resulting from the height difference between the inlet and the end of the outlet tubing. While most of the fluid travels along the main serpentine channel of the device, the small flows across each chamber in the device direct the entry of worms into the single worm loading channel that connect the circular chambers to the serpentine channel (Supplementary Movie 1 and Fig. 1b).

The angle between the loading channel and the serpentine channel is optimized as 20°. Angles that are too large requires worms to bend their body significantly in order to enter, which slows the loading process; angles too small will make fabrication of the wall in between the two channels difficult. The stopper located at the end of the single worm-loading channel restricts the worm from entering the chamber. Once a worm occupies the loading channel, it physically prevents loading of another worm, because the channel has dimensions similar in size to those of a young adult worm.[35] Due to the size variation and high deformability of the animals, occasionally another worm can be partially loaded in the loading channel. However, the mis-loaded worm is efficiently swept out from the loading channel by the flow along the serpentine channel (Supplementary Movie 1).

Once worms are in the loading channels, the large plug is rapidly inserted into the worm inlet (Fig. 2c) to push ~ 100 μl of the buffer solution in the inlet into the serpentine channel and the

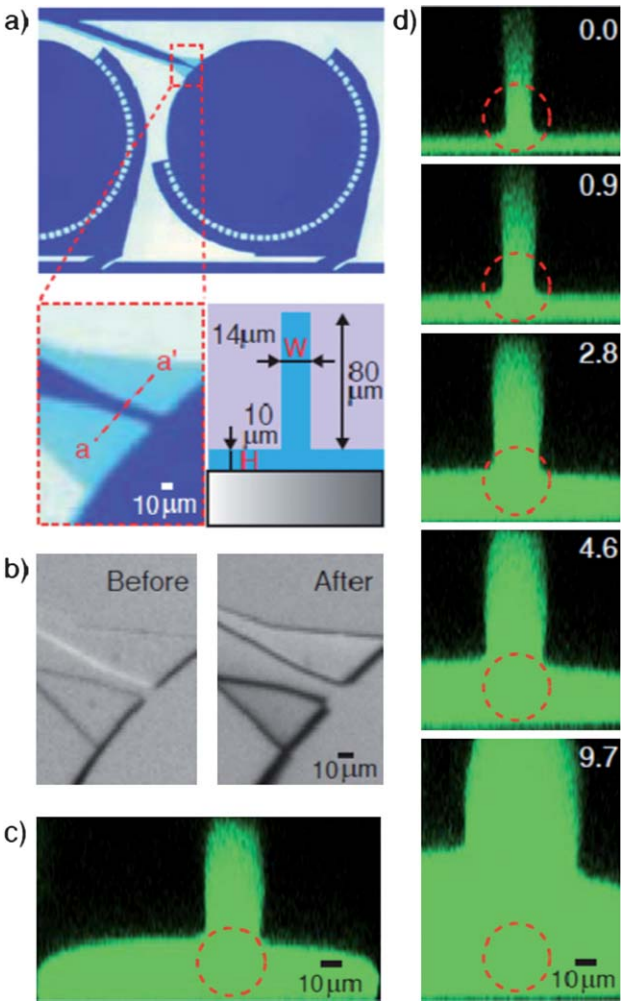

Fig. 4 Expansion of the stopper allows worm loading into the circular chambers. a) Top, optical micrograph of a single chamber; bottom left, zoomed in image of the boxed region showing the stopper; bottom right, schematic of the cross-sectional view (a–a′) of the stopper showing its dimensions. b) Optical micrograph of the stopper before (left) and after (right) the large plug is inserted. c) Confocal image of the cross-section (a–a′) in a showing expansion of the stopper when the large plug is inserted. The outlet valve remained closed. Dotted red circle represents the cross-section of a young adult *C. elegans* (40 μm in diameter). d) Confocal image of the cross-section (a–a′) in a at pressure 0, 0.9, 2.8, 4.6, and 9.7 psi.

chambers. This significantly bulges the highly deformable walls and allows the worms to pass through the stopper into the chambers (Fig. 2c). In this process, an array of small exit channels (diverging channels) ensure a sufficient volumetric flow rate to load worms, but prevent the worms from escaping the chamber by minimizing the exiting flow velocity and shear forces on the worms. The circular chamber isolates worms to avoid physical interaction between individual worms. As shown in the Supplementary Movie 1, the entire worm loading process takes ~ 3 min. Over 17 independent operations of different devices, the average single worm loading success rate was 65%, corresponding to over 30 worms per experiment (Fig. 3). Moreover, 16 out of the 17 trials resulted in 20 or more singly loaded chambers, which is in the range of the sample sizes used in previously published behavioral assays.[24,25] In addition, the operation of the device is simple and does not require any specialized or expensive off-chip components. Therefore, it can be broadly used by non-experts.

Characterization of the deformation of the stopper

The stopper is the key microfluidic component that enables efficient and robust two-step loading of worms while minimizing device complexity. It consists of a wide (100–200 μm), shallow (~10 μm) triangular-shape channel and a narrow (14 μm), tall (~80 μm) channel connected in the middle (Fig. 4a, bottom). This unique three-dimensional structure makes the stopper highly expandable when a small positive pressure change is applied (Fig. 4d). It works as a pressure-sensitive gate to regulate single worm loading in each chamber. During the first step, when worms are loaded in the single worm loading channel, pressure applied to the device is negligible. Under this condition, the cross-section of the stopper is smaller than that of the worm (Fig. 4d, top), and therefore, effectively prevents the animal from loading into the chamber.[35,36] Whereas when ~ 100 μl of buffer solution is rapidly pushed into the device by inserting the large plug, pressure increase in the device expands the stopper enough so that the worm can be pushed into the chamber. As shown in Fig. 4d, when the device is under pressure, the shallow part of the stopper expands upward and the narrow part expands laterally. Together, the cross-section becomes large enough for a worm to pass. To estimate the extent of stopper expansion during actual device operation, we closed the outlet and inserted the large plug. As shown in Fig. 4c, the stopper expands enough for a worm to pass. Although the actual cross-section would be smaller in actual device operation, we observed that essentially every worm in the single worm loading channels was loaded into the chambers (Fig. 3). Furthermore, the opening of the stopper during actual device operation can be tuned by altering the diameter of the large plug or the thickness of the PDMS device. Therefore this design is easily adaptable to experiments on older worms.

Temporal control in chemical delivery

Another advantage of the device is that chemicals can be easily delivered to the chambers in a quick and fully controllable manner. In addition, the delivery of chemicals does not require active external parts or complicated manual manipulation, and only ~50 μl of a solution of the chemical(s) is needed. To deliver chemicals, the small plug is removed and a droplet of chemical

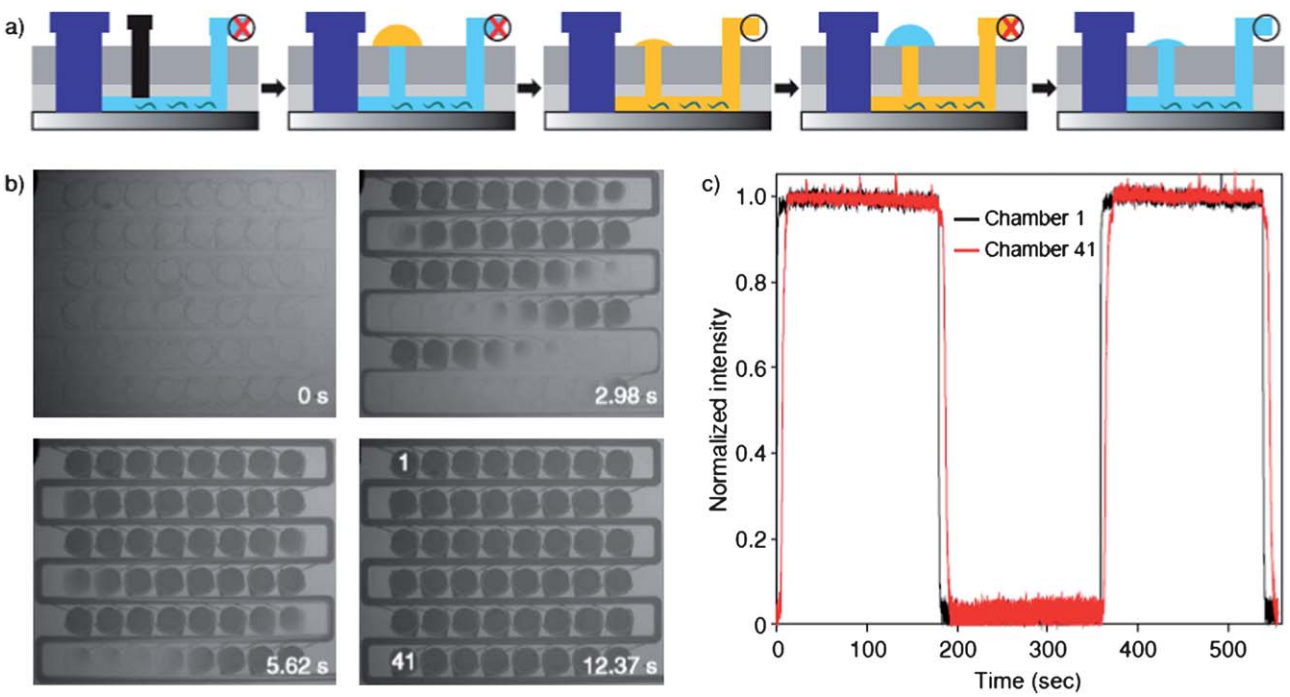

Fig. 5 Easy and controllable chemical delivery. a) Schematic drawing of the cross-section of the device describing the chemical delivery process. b) Optical photographs showing dye delivery. The device reaches a steady state concentration in all chambers in about 13 s. Chamber 41 is the last to reach steady state. The transition time in media exchange can be decreased with increasing flow rates. With observation times of several minutes to an hour, this transition time is often negligible. c) Plot showing stepwise chemical delivery in chamber 1 and chamber 41 as a function of time.

solution (~50 μl in volume) is pipetted on the chemical inlet (Fig. 5a). The small chemical inlet leading into the microfluidic channel has a volume of ~3 μl and minimizes the transition period between assay conditions and the volume of chemical solution needed. As shown in Fig. 5b and c, the device reaches a steady-state concentration in about thirteen seconds (Supplementary Movie 2). The delivery of compounds is also very reproducible in the device (Supplementary Figure 1) and from chamber to chamber (Supplementary Figure 2). Therefore, unlike point source plate assays, where worms are exposed to different environments depending on their position and the effect of chemical gradients cannot be distinguished from the effect of absolute chemical concentration, all the worms in the device experience the same homogenous chemical environment. This significantly reduces experimental error in behavioral assays and allows steady state responses to absolute chemical concentrations to be distinguished from transient responses to concentration changes as the worm travels along the plate.

The transition time between assay conditions also depends on the flow rate and may be decreased by increasing the height difference between the inlet and the outlet. However, with observation times of a couple of minutes to an hour, this transient period is often negligible. In addition, unlike droplet-based microfluidic technology,[19] initial behavioral responses to changing conditions can be monitored because chemical stimuli can be delivered and completely exchanged with new chemical stimuli after worm loading is completed.

Transient response to anesthetic application

To demonstrate the ability of the device to resolve transient behavioral responses to the application of a chemical, we characterized the time-dependent decrease in locomotion after the application of sodium azide. Fig. 6a shows the population average of body bends per second before and after the application of 5 mM and 10 mM sodium azide. Although at both 5 mM and 10 mM concentrations, sodium azide ultimately results in immobilization of all of the worms, our assay allows us to distinguish the two concentrations *via* the speed of immobilization. As expected, 10 mM sodium azide resulted in a much faster rate of decrease in the body bend frequency. However, population means can obscure important aspects of individual worm behavior. The gradual decrease in the average body bend frequency observed in Fig. 6a can be attributed to either gradual decreases in the body bend frequency of each individual worm or sharp decreases in some worms at different times. The ability of our device to track many worms with single worm resolution allows us to obtain longitudinal information for a large number of worms. The raster plots in Fig. 6b and c show, the individual incidences of body bends for each of the 26 worms assayed in both the 5 mM (b) and 10 mM (c) experiments, suggesting that individual worms exhibited a gradual decrease in body bend frequency as well.

In addition to applications in understanding the response time and latent effects of many chemicals, the ability to study initial responses to condition changes may provide mechanistic insights into behaviors such as chemotaxis, where time dependent changes in concentration alter worm locomotion.[18,37–40] Unlike conventional point source plate assays, our device allows precise

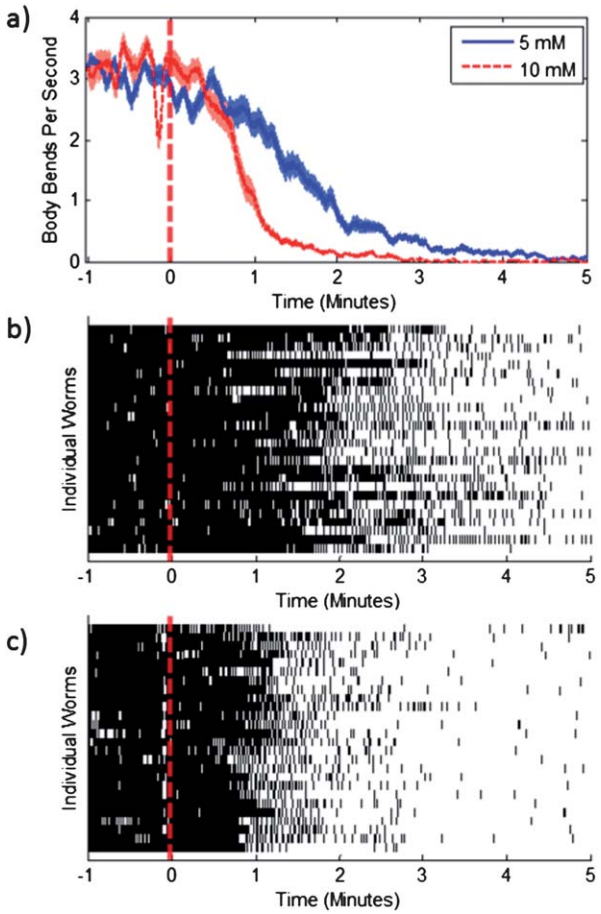

Fig. 6 Quantification of body bending frequency under the influence of sodium azide. a) Population average (n = 26 for both 5 mM and 10 mM conditions) of body bending frequency. Curves represent a 5 s running average of body bend frequency. The standard error for each curve is given in light blue and light red for 5 mM and 10 mM respectively. b) Raster plot showing incidences of body bending for all 26 animals under the influence of 5 mM sodium azide. c) Raster plot showing incidences of body bending for all 26 animals under the influence of 10 mM sodium azide. Red dashed lines indicate the time of sodium azide application (t = 0).

concentration control, temporal control, and permits observation of specific behavioral responses of many animals at a time.

Sex-specific behavioral responses to chemical stimuli

To further demonstrate the capability of the device as a high-throughput chemical screening tool, we utilized the device to study chemical stimuli that elicit sex-specific behavior in *C. elegans.* In many organisms, population-density sensing and sexual attraction rely on small-molecule-based signaling systems.[32,41] In *C. elegans*, media pre-conditioned by young adult hermaphrodites has been demonstrated to be a potent male attractant.[27,28] In most previous studies, male response to conditioned medium was analyzed by measuring time spent within the vicinity of a point source of chemicals placed on an agar plate.[28] Although this attraction assay has been broadly used, it has several limitations. First, the exact concentration of the compounds tested in the scoring region is not well defined, because the chemical diffuses into the agar. Furthermore, the effect of chemical concentration

gradients cannot be distinguished from the effect of absolute chemical concentrations. This can be overcome by adding chemicals to the required concentrations into liquid agar so that the agar plate has uniform chemical concentration throughout. In this assay, reversal frequency of animals on the agar plate can be used as a measure of chemical perception because the frequency correlates with an increase in time spent in the sample-scoring region. However, this assay requires a large amount of chemicals. Second, chemicals cannot be added or removed during assays if they were delivered or incorporated into the agar when the assay plates are made. Third, animals often crawl in and out of the field of view, which makes it difficult to monitor behavioral response with single-worm resolution. Lastly, only a small number of worms can be assayed simultaneously. Our microfluidic device, in comparison, allows monitoring up to 48 individual worms simultaneously. In addition, not only is the exact concentration of the chemical known, but each assay only requires 50 μl of chemicals.

Using the device, we monitored male responses to hermaphrodite-conditioned medium containing the mating signals. Typical *C. elegans* male mating behavior consists of a set of sub-behaviors that include backward locomotion along a hermaphrodite and tight tail-first turns around the hermaphrodite body in search of the vulva.[42] It was observed that in liquid media, male worms exhibit a specific behavior wherein the tail forms a tight coil back on a straightened body. This configuration, heretofore referred to as "male specific behavior" and shown in Fig. 7a, occurs sporadically and persists for periods of several seconds before the worm returns to its normal swimming behavior. Based on preliminary observations of male behavior in our device and prior demonstrations of the male specific effect of hermaphrodite-conditioned medium on solid agar substrate, we hypothesized that exposure to hermaphrodite-conditioned medium would result in a higher incidence of male specific behavior.

Using the procedure outlined in the Experimental section, we exposed *him-5* worms to M9 and young adult hermaphrodite-conditioned medium in succession and measured the percentage of time males engaged in male specific behavior under each condition. Our device facilitated the collection of a large quantity of data where many behavioral readouts, such as body bend frequency, turning frequency as well as other specific body configurations such as the male specific behavior in Fig. 7a, can be tracked for individual worms over a long period of time. To facilitate efficient analysis of a large quantity of data and demonstrate accurate automated determination of behavioral readouts, determination of male specific behavior was performed using custom MATLAB code that detected coiling and body elongation in the worm.[43–45] Validation of our image processing technique against a set of manually annotated images resulted in a specificity of over 99% and a sensitivity of over 94%.

Our results in Fig. 7b show that when subjected to hermaphrodite-conditioned medium, male worms show a significant increase in the percentage of time engaged in male specific behavior ($P < 10^{-6}$). This indicates that chemical signals in

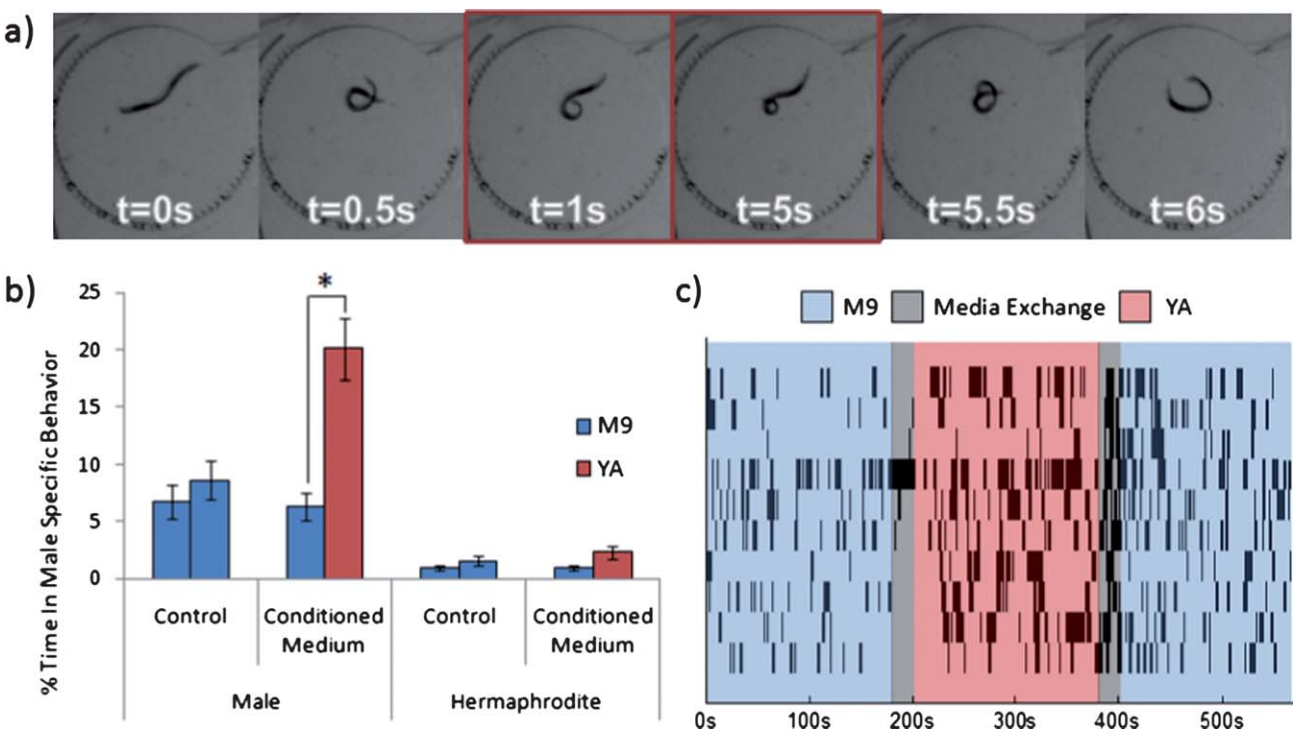

Fig. 7 Quantification of male specific behavior under the influence of hermaphrodite-conditioned medium. a) Time lapse images showing a worm entering into, maintaining and exiting out of male specific behavior. Frames categorized as male specific behavior are outlined in red. b) Quantification of the percentage of time engaged in male specific behavior for males and hermaphrodites subjected to sequential treatment of M9 and M9 or M9 and YA (young adult conditioned medium). n = 16 for male control, n = 35 for male conditioned medium, n = 20 for hermaphrodite control, n = 19 for hermaphrodite-conditioned medium. *Statistically significant $P < 10^{-6}$. Other data pairs are not statistically significant ($\alpha = 0.05$). c) Raster plot showing incidences of male specific behavior for 10 male worms during a full experiment (3 min M9, 3 min conditioned medium, 3 min M9).

hermaphrodite-conditioned medium trigger a specific behavioral response in male worms other than locomotive behavior such as forward moving and pirouettes.[37–40] Unlike assaying dwell times on plate, our device provides the means to easily dissect out specific components of behavioral response. This opens up exciting opportunities in ascertaining the specific behavioral effect of individual chemicals in complex mixtures such as hermaphrodite-conditioned medium. Unlike males, hermaphrodites were very rarely observed to engage in male specific behavior in the assays (Fig. 7b).

Similar to individual tracking in the assays with anesthetics, Fig. 7c shows a representative selection of individual worm behavior in response to conditioned medium. With high time resolution for many individual worms, we observe that an increase in the incidence of male specific behavior happens within ~30 s of introducing the conditioned medium. Interestingly, we also find that a less pronounced increase in the incidence of male specific behavior persists after conditioned medium has been replaced with M9. This may indicate that decreasing concentrations of the hermaphrodite-derived stimulus also trigger male-specific behavior, as opposed to possible adsorption of compounds in the PDMS walls (Supplementary Figure 3).

Conclusions

We have reported here a microfluidic device that allows for the behavior tracking of single worms and delivery of stimuli with precise temporal control. Using this microfluidic chamber array, we were able to study the behavioral response of a large number of individual worms to drugs and sex pheromones in hermaphrodite-conditioned medium. Unlike previously reported methods for chemical response assays, our method permits the simultaneous longitudinal investigation of large numbers of freely moving worms and allows for excellent temporal control in the delivery of chemicals. Because the working principle of the system allows simple parallelization, the throughput can be further improved. Furthermore, this device can also be used to observe behavior responses to thermal and light stimuli. We envision that this system will greatly facilitate numerous chemical screening studies on *C. elegans* including neurodegenerative disorders, diabetes, addiction, and aging related diseases.

Notes and references

1 J. T. Shin and M. C. Fishman, *Annu. Rev. Genomics Hum. Genet.*, 2002, **3**, 311–340.
2 D. St Johnston, *Nat. Rev. Genet.*, 2002, **3**, 176–188.
3 E. Bier, *Nat. Rev. Genet.*, 2005, **6**, 9–23.
4 M. Vidal and R. L. Cagan, *Curr. Opin. Genet. Dev.*, 2006, **16**, 10–16.
5 D. J. Grunwald and J. S. Eisen, *Nat. Rev. Genet.*, 2002, **3**, 717–724.
6 G. J. Lieschke and P. D. Currie, *Nat. Rev. Genet.*, 2007, **8**, 353–367.
7 A. K. Jones, S. D. Buckingham and D. B. Sattelle, *Nat. Rev. Drug Discovery*, 2005, **4**, 321–330.
8 T. Kaletta and M. O. Hengartner, *Nat. Rev. Drug Discovery*, 2006, **5**, 387–398.
9 S. Brenner, *Genetics*, 1974, **77**, 71–94.
10 J. G. White, E. Southgate, J. N. Thomson and S. Brenner, *Philos. Trans. R. Soc. London, Ser. B*, 1986, **314**, 1–340.
11 C. I. Bargmann, E. Hartwieg and H. R. Horvitz, *Cell*, 1993, **74**, 515–527.
12 M. Chalfie, Y. Tu, G. Euskirchen, W. W. Ward and D. C. Prasher, *Science*, 1994, **263**, 802–805.
13 A. Fire, S. Xu, M. K. Montgomery, S. A. Kostas, S. E. Driver and C. C. Mello, *Nature*, 1998, **391**, 806–811.
14 S. Ward, *Proc. Natl. Acad. Sci. U. S. A.*, 1973, **70**, 817–821.
15 D. B. Dusenbery, *J. Comp. Physiol.*, 1980, **136**, 327–331.
16 R. Kerr, V. Lev-Ram, G. Baird, P. Vincent, R. Y. Tsien and W. R. Schafer, *Neuron*, 2000, **26**, 583–594.
17 W. S. Ryu and A. D. T. Samuel, *Journal of Neuroscience*, 2002, **22**, 5727–5733.
18 L. Luo, C. V. Gabel, H. I. Ha, Y. Zhang and A. D. T. Samuel, *J. Neurophysiol.*, 2008, **99**, 2617–2625.
19 W. W. Shi, J. H. Qin, N. N. Ye and B. C. Lin, *Lab Chip*, 2008, **8**, 1432–1435.
20 T. V. Chokshi, D. Bazopoulou and N. Chronis, *Lab Chip*, 2010, **10**, 2758–2763.
21 S. E. Hulme, S. S. Shevkoplyas, A. P. McGuigan, J. Apfeld, W. Fontana and G. M. Whitesides, *Lab Chip*, 2010, **10**, 589–597.
22 C. B. Rohde, F. Zeng, R. Gonzalez-Rubio, M. Angel and M. F. Yanik, *Proc. Natl. Acad. Sci. U. S. A.*, 2007, **104**, 13891–13895.
23 J. A. Carr, A. Parashar, R. Gibson, A. P. Robertson, R. J. Martin and S. Pandey, *Lab Chip*, 2011, **11**, 2385–2396.
24 P. T. McGrath, M. V. Rockman, M. Zimmer, H. Jang, E. Z. Macosko, L. Kruglyak and C. I. Bargmann, *Neuron*, 2009, **61**, 692–699.
25 E. Z. Macosko, N. Pokala, E. H. Feinberg, S. H. Chalasani, R. A. Butcher, J. Clardy and C. I. Bargmann, *Nature*, 2009, **458**, 1171–1175.
26 L. Rivard, J. Srinivasan, A. Stone, S. Ochoa, P. Sternberg and C. Loer, *BMC Neurosci.*, 2010, **11**, 22.
27 J. M. Simon and P. W. Sternberg, *Proc. Natl. Acad. Sci. U. S. A.*, 2002, **99**, 1598–1603.
28 J. Srinivasan, F. Kaplan, R. Ajredini, C. Zachariah, H. T. Alborn, P. E. A. Teal, R. U. Malik, A. S. Edison, P. W. Sternberg and F. C. Schroeder, *Nature*, 2008, **454**, 1115–U1146.
29 C. Pungaliya, J. Srinivasan, B. W. Fox, R. U. Malik, A. H. Ludewig, P. W. Sternberg and F. C. Schroeder, *Proc. Natl. Acad. Sci. U. S. A.*, 2009, **106**, 7708–7713.
30 J. W. Golden and D. L. Riddle, *Science*, 1982, **218**, 578–580.
31 J. W. Golden and D. L. Riddle, *Proc. Natl. Acad. Sci. U. S. A.*, 1984, **81**, 819–823.
32 C. Dulac and A. T. Torello, *Nat. Rev. Neurosci.*, 2003, **4**, 551–562.
33 J. Q. White, T. J. Nicholas, J. Gritton, L. Truong, E. R. Davidson and E. M. Jorgensen, *Curr. Biol.*, 2007, **17**, 1847–1857.
34 D. C. Duffy, J. C. McDonald, O. J. A. Schueller and G. M. Whitesides, *Anal. Chem.*, 1998, **70**, 4974–4984.
35 K. Chung and H. Lu, *Lab Chip*, 2009, **9**, 2764–2766.
36 K. H. Chung, M. M. Crane and H. Lu, *Nat. Methods*, 2008, **5**, 637–643.
37 J. T. Pierce-Shimomura, T. M. Morse and S. R. Lockery, *J Neurosci*, 1999, **19**, 9557–9569.
38 J. T. Pierce-Shimomura, M. Dores and S. R. Lockery, *J. Exp. Biol.*, 2005, **208**, 4727–4733.
39 A. C. Miller, T. R. Thiele, S. Faumont, M. L. Moravec and S. R. Lockery, *J. Neurosci.*, 2005, **25**, 3369–3378.
40 Y. Iino and K. Yoshida, *J. Neurosci.*, 2009, **29**, 5370–5380.
41 A. Camilli and B. L. Bassler, *Science*, 2006, **311**, 1113–1116.
42 M. M. Barr and L. R. Garcia, *WormBook*, 2006, 1–11.
43 C. Cronin, J. Mendel, S. Mukhtar, Y.-M. Kim, R. Stirbl, J. Bruck and P. Sternberg, *BMC Genet.*, 2005, **6**, 5.
44 K. Hoshi and R. Shingai, *J. Neurosci. Methods*, 2006, **157**, 355–363.
45 K.-M. Huang, P. Cosman and W. R. Schafer, *J. Neurosci. Methods*, 2006, **158**, 323–336.